Effects of container geometry on granular convection

E. L. Grossman*
The James Franck Institute, The University of Chicago, 5640 South Ellis Avenue, Chicago, Illinois 60637
(Received 26 February 1997)

In this work we use computer simulations to examine the effects of boundary conditions on convection in vibrated granular systems. A two-dimensional model reproduces experimental results on the form of the convective velocities and the reversal of the convection rolls. We then look in detail at the role of the wall preparation and discuss a possible mechanism to account for the range of observed behaviors. [S1063-651X(97)09109-5]

PACS number(s): 81.05.Rm, 46.10.+z, 47.27.Te, 05.40.+j

I. INTRODUCTION

Granular systems are everywhere. From the powders used by pharmaceutical companies to the boulders that comprise rock slides, granular materials of all shapes and sizes influence our lives. Many people wish to predict and control the behavior of large ensembles of such particles. An important question that arises in many contexts is how granular materials respond to shaking. Whether this vibration is purposeful, designed to produce a mixture of two species, or accidental, resulting from the motion of a railway car or a tractor trailer, the effects of the oscillations can vary widely. Some of the variables include the material being shaken, the strength of the shaking, and the container in which the shaking occurs. In this paper, we focus mainly on the last factor: the shape and surface preparation of the vessel that holds the vibrated granular material.

Experiments have demonstrated that shaken granular systems can exhibit a wide range of behaviors such as fluidization, surface waves, convection, and compaction [1,2]. Here we study convection, which has been examined in connection with heaping [3,4] and size separation [5]. In this work, we focus not on the effects of convection, but on its causes.

Two experimental papers [6,7] provide a great deal of quantitative information about granular convection. The goal of this work is to simulate the systems studied, reproduce the experimental results, and use the computational systems to gain insight into the physical mechanisms at work. When a granular material is driven at the right strength, convection results. This motion is usually observed for accelerations ranging from one to ten times gravity. Lesser forcing leads to compaction, while stronger driving produces period-doubling behavior [7–10], bubbling [11], or total fluidization, although the size and aspect ratio of the granular bed, as well as the material used, have a large effect on what behavior occurs under which conditions.

For a container with rough vertical walls and an aspect ratio of order one, the convection rolls are such that particles move up the center of the container in a wide swath and down the sides in narrow bands. Conservation of particle flux implies that the upward motion is therefore slower than the downward motion. This sort of behavior will be referred to in this paper as a ''normal roll.'' In containers where the walls have been tilted outward, motion can be seen in which the particles move down in the center of the container and up along the sides. This will be called a ''reversed roll.'' We are interested in what conditions produce this second sort of behavior and how the transition between the two types of rolls occurs.

Therefore, the simulations are designed to allow us to look at a granular material in a variety of enclosures. The system in question is a two-dimensional model of the experiments (see Fig. 1). There is a container with a base and walls. The walls can be vertical or rotated out at some angle θ. The base is smooth, but the side walls have half spheres of diameter d_w glued to them at random intervals. The free grains are spheres with average diameter d. The whole container is shaken up and down with frequency f and amplitude A. The strength of the driving is characterized by Γ, the ratio of the container's acceleration to gravity. As the aim of this paper is to recreate experimental systems, parameters were chosen to match those used in the experiments. This fixed the size of the particles and the frequency of the oscillations (see Table I).

It has been noted that the shape of the container in which

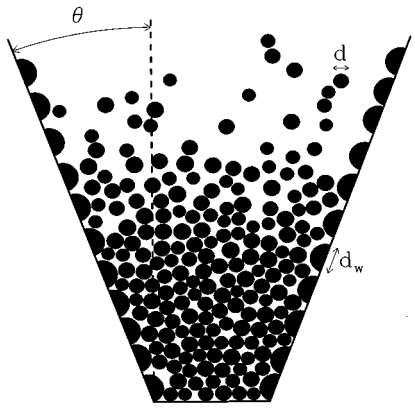

FIG. 1. Picture of the system. The average diameter of the free particles is d and the diameter of the particles affixed to the walls is d_w (here $d_w/d=2$). The angle that the walls form with the vertical is given by θ (here $\theta=20°$). The whole container oscillates with amplitude A and frequency f. The coordinate system used in this paper is (r,z), where z is the height above the base and r is the horizontal distance from the center of the container.

*Electronic address: grossman@cs.uchicago.edu

TABLE I. Physical parameters used in the simulations.

Particle characteristics	average diameter $(d)=0.9$ mm variation in $d=\pm 0.1$ mm
Wall characteristic	$\theta=0°-25°$; wall particle diameters $(d_w/d)=0.25, 0.5, 1.0, 2.0$
Forcing parameters	$\Gamma=7,8$ $f=20, 25, 30$ Hz
Collison parameters	$\epsilon_n=0.97$, $\epsilon_t=0.44$, $\mu=0.092$ $\epsilon_n^w=0.831$, $\epsilon_t^w=0.31$, $\mu^w=0.125$

the granular material is being shaken as well as the condition of the surfaces of the container can materially effect the behavior. Therefore, the main characteristics that we will vary are the angle of the sidewalls with the vertical (θ) and the sidewall roughness, as quantified by the ratio of the diameter of the particles glued to the wall to the average diameter of the freely moving particles (d_w/d).

II. MODEL FOR COLLISIONS

In this work, we examine a two-dimensional granular system as modeled on a computer. The particles used are spheres of varying sizes but constant density. There are two key characteristics of granular systems. First, there are no interparticle forces; the only way one grain can interact with another is through physical contact: a collision. Second, such collisions are inelastic; energy is lost. Thus, as a whole, granular systems are dissipative. There are a variety of theories used to simulate such collisions [12,13], but we have chosen to use the modification of Maw, Barber, and Fawcett's model that was proposed by Walton [14] and tested by Foerster, Louge, Chang, and Allia [15]. The advantage of this choice is that it allows for particle rotation and includes frictional effects, which have both been recognized as key elements in granular convection [16].

This is a completely deterministic model; in a collision, the final velocities of the particle are unique functions of the initial velocities and the three constants used to parametrize the degree of inelasticity and friction of the particle-particle interaction. The first parameter ϵ_n is the normal coefficient of restitution. This parameter, in some guise, appears in almost all models. It represents the energy loss into heat due to deformation of the particles during a collision. Quantitatively, it is the factor by which the component of the relative velocity normal to the plane of collision (e.g., parallel to the line between the centers of the colliding particles) is reduced:

$$v_n^{rel\prime}=-\epsilon_n v_n^{rel},$$

$$v_n^{rel}\equiv v_{n1}-v_{n2}, \tag{1}$$

where unprimed quantities describe the system before the collision and primed quantities are for after. The negative sign in front of ϵ_n indicates that while before the collision the particles are moving toward each other and the normal relative velocity (v_n^{rel}) is negative, afterward, they are separating and $v_n^{rel\prime}$ will be positive.

The interaction of surfaces in contact are described by two regimes: one determined by the coefficient of static friction, one by the coefficient of sliding friction. Therefore, Walton's model assumes that including friction results in two types of collisions: sticking and sliding. In the former kind, the behavior of the tangential relative velocity at the point of contact is modeled in the same way as the normal relative velocity:

$$v_t^{rel\prime}=-\epsilon_t v_t^{rel},$$

$$v_t^{rel}\equiv(v_{t1}-r_1\omega_1)-(v_{t2}+r_2\omega_2), \tag{2}$$

where v_t is the tangential component of the linear velocity and $r\omega$ is the contribution of the rotational motion. Equations (1) and (2), coupled with the requirements of momentum conservation, are enough to determine the postcollision velocities $(\vec{v}_1',\vec{v}_2',\omega_1',\omega_2')$ of the particles in terms of the initial conditions $(\vec{v}_1,\vec{v}_2,\omega_1,\omega_2)$ and the collision parameters ϵ_n and ϵ_t.

For sliding collisions, the behavior can be calculated using the traditional coefficient of sliding friction μ. Here the force in the tangential direction has a magnitude proportional to the force in the normal direction and is directed so as to reduce the magnitude of the tangential relative velocity. Specifically,

$$F_t=-\mu F_n\ \mathrm{sgn}(v_t^{rel}), \tag{3}$$

where F_t and F_n are the forces exerted on particle 1 by particle 2 and are related to the velocities through conservation of momentum, e.g., $F_n=m_1(v_{n1}'-v_{n1})=-m_2(v_{n2}'-v_{n2})$. In fact, this model assumes instantaneous collisions, so technically F_n and F_t are actually impulses. (A further discussion of the implications of the assumption of infinitesimal collision times occurs later in this section.) Thus, again, the final velocities can be calculated as a function of the initial velocities and the two collision parameters, this time ϵ_n and μ.

The remaining detail of the model is how one determines whether an interaction is a sticking or a sliding collision. For relative velocities with small tangential components, the static contact point of the sticking model (using ϵ_t) describes the behavior. For relative velocities with large tangential components, the frictional sliding motion (using ϵ_n) is more appropriate. Thus, assuming that they do not coexist and the transition between the types of behavior is a smooth one, the crossover point should occur at the relative velocity for which both models give the same prediction. Quantitatively, this condition can be expressed as

$$\frac{-v_n^{rel}}{|v_t^{rel}|}>v_{ratio}^{trans}\rightarrow \text{ sticking}, \tag{4}$$

$$\frac{-v_n^{rel}}{|v_t^{rel}|}<v_{ratio}^{trans}\rightarrow \text{ sliding},$$

$$v_{ratio}^{trans} \equiv \frac{(1+\epsilon_t)}{\mu(1+\epsilon_n)(1+1/I_c)},$$

where v_n^{rel} and v_t^{rel} are as defined in Eqs. (1) and (2), ϵ_n, ϵ_t, and μ are the collision parameters, and I_c is the prefactor in the moment of inertia of the colliding particles (i.e., $I_c=2/5$ for spheres or $I_c=1/2$ for disks). With this condition, the models for sticking and sliding collisions described above, and conservation of linear and angular momentum, the final velocities for any set of initial conditions are now well defined. Note that the positions of the particles are unimportant except in the determination of the normal and tangential directions. This model can be extended to describe particle-wall collisions: The wall is treated as a particle with infinite radius. If the wall is made of a different material from the particles, there is no reason to expect the collision parameters to be the same.

Parameters and assumptions of the simulations

Experiments on granular convection are usually done with hard particles, such as glass beads or steel balls or poppy seeds. In order to ensure that the collision parameters accurately represent experiment particles, we turn to Foerster *et al.* [15]. They observed binary collisions between soda lime glass spheres as well as collisions between the spheres and an aluminum plate. From their data, values of the collision paramenters were deduced. These values were used in this paper's computational work in order to ensure that the model in simulations was physical and mimicked the type of particles used in convection experiments (see Table I).

In general, the simulations were designed to match the experiments whenever possible. However, certain concessions were made to computational limitations. For example, the forcing was not sinusodial or sawtooth as has been used in other computational work [4,17], but rather a series of linked parabolas. Thus the velocity of the container changes continuously, but its acceleration does not (see Fig. 2). The parabolic form enables the point of interception between the base and a falling particle to be calculated exactly and makes the simulations faster and more accurate. Another difference is that the while the model can be applied (and the experiments of Foerster *et al.* are carried out) in three dimensions, the simulation is strictly two dimensional. This does not preclude comparison to experimental systems, as the opacity of granular materials often leads scientists to study systems that are many particle diameters high and wide, but only at most several particle diameters deep. In this work, the simulations will be compared to such quasi-two-dimensional systems, as well as to three-dimensional experiments. The final concession made to computer time limitations was to occasionally force simulated systems more strongly (at slightly higher Γ) than the experimental systems were driven.

A major characteristic of the model chosen for these simulations is the assumption that collisions occur instantaneously. Actually, this is equivalent to asserting that the time for which the particles are in contact is much less that any other time scale in the problem, specifically, much less than the average time between collisions. This is valid for a collection of very hard particles. Such spheres undergo very little compression during a collision, so the contact time is

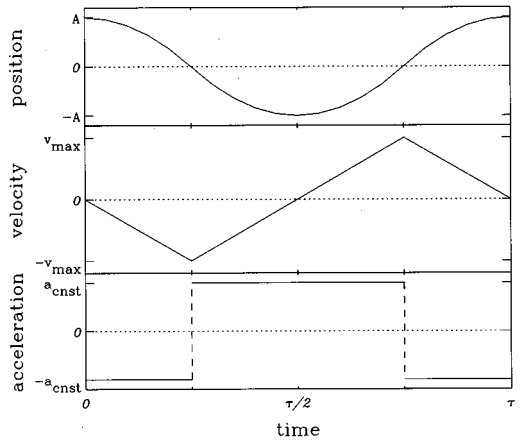

FIG. 2. Motion of the base of the container over the course of a cycle. The free parameters are the amplitude (A) of the oscillation and the frequency (f) or, equivalently, the period ($\tau=1/f$). The base trajectory is a series of parabolas. Thus the velocity varies linearly between $\pm v_{max}$, where $v_{max}=8Af$, and the acceleration has a constant magnitude of $a_{const}=32Af^2$. Thus the normalized acceleration is $\Gamma=32Af^2/g$, where g is the gravitational acceleration at the surface of the Earth.

short. Implicit in this view is that for hard particles, the normal coefficient of restitution ϵ_n is very close to unity. Since little compression occurs, very little energy is converted to heat so, at least in the normal direction, the particles are nearly elastic.

When the collision time is assumed to be zero, the system can be simulated using an event-driven (ED) code, a common technique for computational studies of granular systems [18,19]. Another method is to use soft particles in a molecular-dynamics code [4,20]. Each approach has its benefits and costs, but it has been established that for hard particles, ED simulations are both more efficient and more accurate [12,21]. The main concern for such an approach is the possibility of inelastic collapse [22,23]. This phenomenon occurs when the time between collisions goes to zero and the system undergoes an infinite number of collisions in a finite time. How many particles are involved in the collapse depends on the density of the system and the values of the collision parameters. The ''stickier'' the system (i.e., the more energy lost per collision), the more likely inelastic collapse. The physical configuration of the particles involved also plays a large part in determining whether a cluster of grains will collapse or merely collide many time before moving apart [24,25]. This influence of geometry led Deltour and Barrat to propose a mechanism to avoid collapse [26]. They suggest that if they introduce a small random rotation in the final velocities after each collision, the structures necessary for collapse will have difficulty forming. This approach is justified by invoking the ''surface roughness'' of real particles and, as they demonstrate, does succeed in retarding or even repressing inelastic collapse. Although this method disturbs conservation of momentum at the level of individual collisions, in a system without directional bias, the global effects of this perturbation should average out. However, in systems such as the ones studied in this paper, where gravity and external forcing break the symmetry so that all collisions are not equivalent, this approach acts to feed momentum in a

certain direction into the system; the changes in momentum due to the random rotations do not average out over time. Also, inelastic collapse can occur not only among particles, but also between particles and a wall. In that case, geometry is less important, so the rotation will not have the same effect. Therefore, for the simulations in this paper, when inelastic collapse threatened to stop the computation, one of the particles involved was given a small jolt of energy (the magnitude of its linear velocity was multiplied by a factor slightly larger than one) in order to break up the cluster. For the collision parameters chosen, this was seldom an issue; the technique was needed perhaps once in every 10^6 collisions. On these few occasions that it was used, the ''jolt'' method successfully prevented collapse.

III. CONTAINERS WITH VERTICAL WALLS

Magnetic resonance imaging (MRI) has been used to look at the flow patterns of granular materials in a variety of geometries [27,28]. Specifically, Knight *et al.* [6] have conducted detailed studies of normal convection rolls in a cylindrical container filled with poppy seeds. The base of the container is smooth, but there are seeds glued to the vertical walls. MRI enables them to measure convective velocities throughout the container. The same quantities can be calculated for the simulational systems, and the magnitudes and the functional dependences on depth or radial coordinate can be compared with the experiment.

Throughout this paper, the velocity profiles discussed do not refer to the actual motion of a particle at a given moment in time. Instead, we measure the net displacement of a particle after one complete oscillation. As the container rises and falls, the particle may explore a wide range of space, but the change in the average position of a particle at a fixed point in the cycle is what defines convective motion. An example of how the particles shift over the course of one oscillation of the container is shown in Fig. 3. These are snapshots of the system before and after one shake. There is no difference between the dark and light particles; they are just colored that way for visual effect. Note that in the middle of the container there is slow, coherent flow upward, while at the edges, the motion is downward, faster, and more scattered. This is normal convection, like that seen in experiments.

By averaging the net displacements per cycle over many particles and many shakes, the simulational convective velocities can be calculated and compared to those observed in three-dimensional systems using MRI. Note that the simulations and the experiments use the same technique to determine the velocity profiles. The results are qualitatively identical and quantitatively very similar. The experimental work [6] demonstrates that the flow profiles vary exponentially with height and that the radial dependence of the velocity can be described by a hyperbolic cosine [29]. The data from the simulations are shown in Fig. 4. The height dependence deviates from exponential near the top and the bottom of the bead pack; the same sort of deviations are seen in the experiments. For the radial dependence, the simulations were performed in three containers of varying sizes. We have fit both parabolic and hyperbolic cosine functions to the data. The former is what might be expected for flow of a liquid through a narrow pipe; here it is inadequate to describe the convection velocity function. Both the simulations and the experiments measure convection velocities on the order of a particle diameter per cycle. This implies that a grain might take approximately 50 shakes to move from the base of the container to the top surface. A final point of agreement between the experiments and the simulations is the enlargement of the downward flowing region near the walls as the size of the container increases [this trend can be deduced from the data in Fig. 4(b)]. If the size of this region scales with the size of the system, we expect convection to persist even as the system grows very large [6].

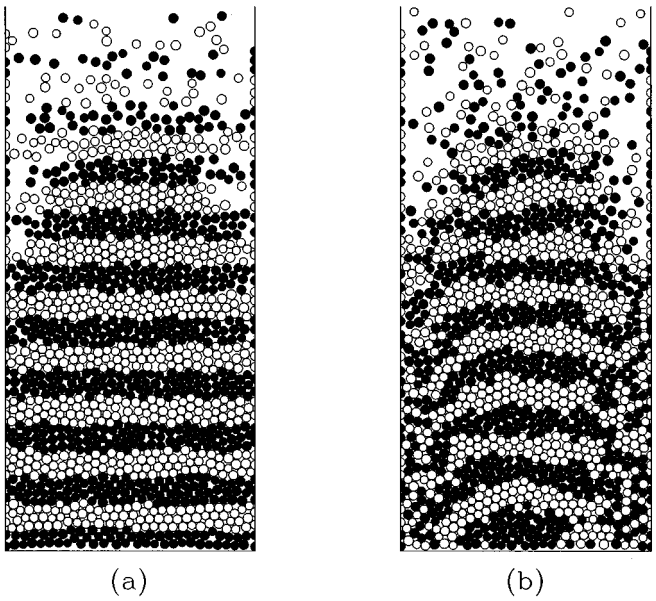

FIG. 3. Position of the grains (a) before and (b) after one shake. The container is $28.22d$ wide and the filling height is approximately $45d$. The half spheres glued to the wall have a diameter equal to the average diameter of the free particles ($d_w/d = 1.0$). The frequency is 20 Hz and the amplitude is 6.8 particle diameters, so $\Gamma = 8.0$.

One of the observed consequences of normal convection is the formation of a heap on the top surface of the granular bed. Experimentalists have identified two important factors that affect the size and existence of such a heap: the ambient gas pressure [30] and the friction between particles [31]. Since interparticle gas molecules are not included in computational models of granular systems, heaping is more difficult to observe in simulations [32,33]. In this work, the collision model contains friction and thus in theory heaping could be observed. In fact, there does seem to be a curve along the top surface of the granular pile in Fig. 3. However, because most of the systems studied in this paper do not have a well-defined top surface, in general heaping was not observed. The absence of a distinct top to the granular pile is due to the small size of the computational systems. In vibrated granular systems, the energy input occurs mainly at the base of the container. Collisions transfer the energy up through the bead pack. Since the collisions are inelastic, energy is continually dissipated during this process. In large or very inelastic or weakly forced systems, all of the driving energy can be dispersed among the particles or lost through collisions. But if the system is unable to absorb all of the input energy, the

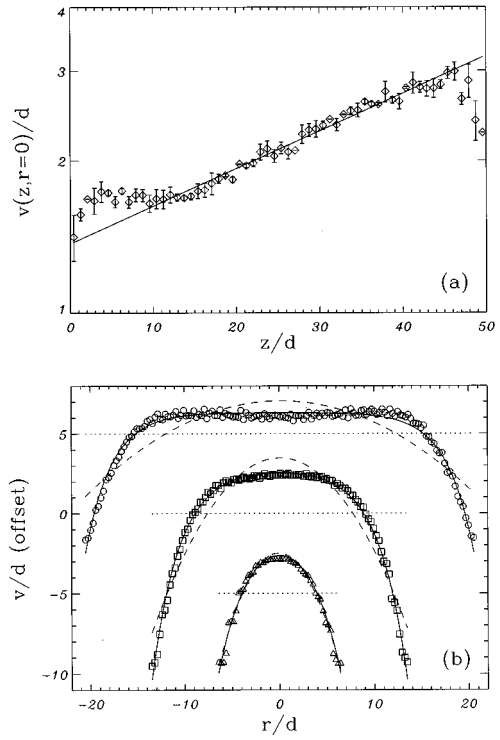

FIG. 4. Convection velocity. This is defined as the displacement of a grain over the course of a cycle in units of particle diameters. These data are all for $\Gamma = 8.0$. (a) The height dependence in the center of a container of width $14.11d$. (b) The radial dependence for containers of widths $14.11d$ (triangles), $28.22d$ (squares), and $42.33d$ (circles). The data for the first two was taken $22.5d$ above the base, while the last was taken $12.25d$ above the base. The data were fitted to a hyperbolic cosine (solid line) and a parabolic function (dashed line). Note that, for clarity, the data have been offset. The dotted lines identify the zero axis for each set of data. Note that d, z, and r are defined in Fig. 1.

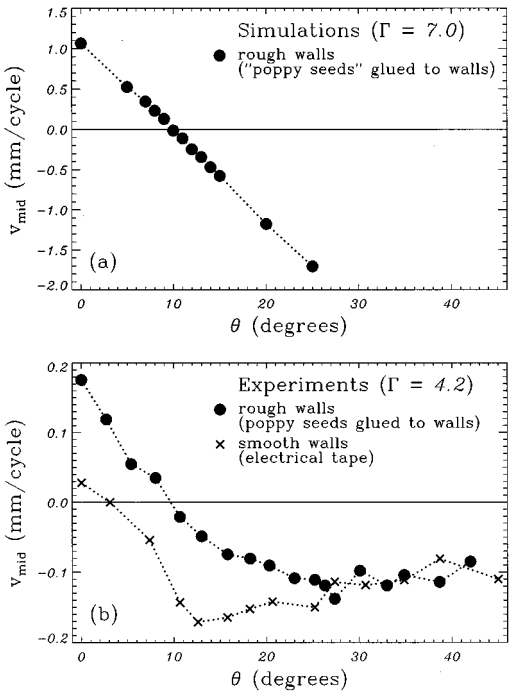

FIG. 5. Convection velocity (v_{mid}) of particles in the center of the container as a function of wall angle (θ). The velocities are in millimeters per cycle. (a) Data from the simulations. Note that the transition between normal and reversed rolls occurs at the angle for which $v_{mid} = 0$; therefore $\theta_{tr} = 10°$. The system is $15d$ wide at the base with a filling height of $23d$. The frequency is 25 Hz and the amplitude is $3.81d$, so $\Gamma = 7$. The walls are rough, i.e., there are particles identical to the free particles glued to the walls. (b) Data from the experiments, courtesty of Knight. The solid circles are the data for rough walls (poppy seeds glued to them) and can be compared to the simulational data in (a). Note that the transition angle is again 10°. Here the system is approximately 50×50 particle diameters and the container is shaken with $\Gamma = 4.2$ (the frequency is again 25 Hz). The weaker forcing in the experiments explains why the magnitude of the convective velocities is smaller in the experiments than in the simulations. The crosses are data from the same experimental system, but the walls in this case have been covered with electrical tape to make them smoother.

particles at the top of the bead pack will receive a disproportionate amount of energy and the uppermost layers of the system will become fluidized [10]. Since the computational systems studied in this work used hard (not very inelastic) particles and were on the small side ($15d \times 23d$), this fluidization occurred, a top surface could not be defined, and hence heaping could not be observed.

IV. PIVOTING THE WALLS

The preceding section examined the motion of a granular material in a container with vertical walls, i.e., $\theta = 0$. This section looks at how these normal convection rolls are altered as the walls of the container are rotated outward ($\theta > 0$). The goal is to look at the direction and strength of the convection rolls at a variety of wall angles. To quantify these characteristics, we will measure the convective velocities (v_{mid}) of the particles in the center of the container. The direction of the convection rolls can then be determined from the sign of v_{mid}: If the middle particles are moving upward ($v_{mid} > 0$), there are normal convection rolls, but if the particles in the center are moving down ($v_{mid} < 0$), then the rolls are reversed. Therefore, the transition angle θ_{tr} is the value of θ at which $v_{mid} = 0$; for $\theta < \theta_{tr}$, the rolls are normal, and for $\theta > \theta_{tr}$, they are reversed. The magnitude of v_{mid} also gives a sense of the strength of the convection. Note that this is the same technique employed in the experiments [7].

Simulations were performed for a container that was $15d$ wide at the base and filled to approximately $23d$. (This system is about half as tall and a third as wide as the one used in the experiments.) The frequency is 25 Hz and the amplitude is 3.81 particle diameters, so the normalized acceleration Γ is equal to 7.0. The walls are covered with particles just like the free particles. Figure 5(a) shows the data from the simulations at wall angles between 0° and 25°. Note that strong normal rolls are observed for vertical walls ($\theta = 0$), while strong reversed rolls can be seen at large wall angles. At intermediate angles, the rolls are weaker and the transition from normal to reversed rolls occurs at approximately 10°.

Figure 5(b) shows the experimental results [7] for a similar system. Note that, again, the transition angle is 10°. The measured convective velocities are of the same order of mag-

nitude in both systems. They are not identical, as there are some differences between the simulations and the experiment. The particles are the same size and the frequency is the same; however, due to computational limitations, the strength of the forcing is higher for the computational system ($\Gamma = 7.0$ instead of $\Gamma = 4.2$). This explains why the magnitudes of v_{mid} are larger in the simulations. There is experimental evidence to suggest that the value of the transitional angle is independent of Γ, so the reproduction of the experimental value of θ_{tr} by the simulations is a valid confirmation of the computational approach. It is important to emphasize that the wall preparations in the simulations and the experiments are identical.

V. WALL PREPARATION

Many previous works have emphasized the importance of the wall-particle interaction in granular convection. Specifically, both experimental and computational results [4,5,20,31,32,34] indicate that changing the frictional character of the wall can have quantifiable effects on the magnitude of the convection in a container with vertical walls. In addition, Knight's experiments on convection in containers with tilted out walls [7] examine the effects of smoothing the walls at a variety of wall angles. His results demonstrate that putting electrical tape on the walls, instead of gluing particles there, almost totally suppressed the normal convection rolls and thus moved the transition angle close to zero ($\theta_{tr} = 3°$); see Fig. 5(b). Computationally, it is difficult to know exactly how to model the interactions between the poppy seeds and the electrical tape. However, the dependence on wall roughness in the simulations can be tested by varying the size of the particles attached to the walls. When these wall particles are much smaller than the free grains ($d_w/d \ll 1$), the surface appears smooth, while if they are much larger ($d_w/d \gg 1$), it seems rough. Figure 6(a) shows the behavior at various angles for $d_w/d = 0.25$, 0.5, 1.0, and 2.0. From these data, two trends are clear. First, for vertical walls ($\theta = 0$), the rougher walls produce stronger convection (the convective velocity is larger). Second, the smoother walls must in some way enhance the formation of reversed rolls, as the systems with smoother walls have lower transition angles. This result is summarized in Fig. 6(b). These two trends are also observed in the experimental data [see Fig. 5(b)]. Note, however, that simulations were not performed at larger angles ($\theta > 25°$), so certain experimental behaviors, such as the convergence of the convection velocities for rough and smooth walls at high θ, are not discussed in this work.

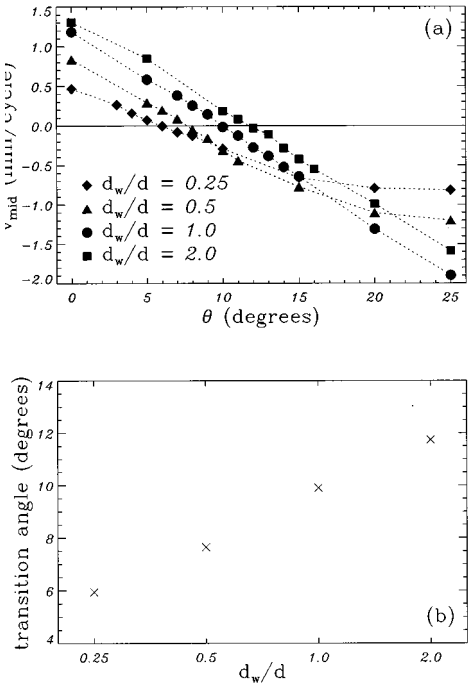

FIG. 6. (a) Convection velocities (v_{mid}) of particles in the center of the container as a function of wall angle (θ) for various wall preparations. Roughness is parametrized by the ratio of the diameter of the wall particles to that of the free particles (d_w/d); smoother walls have lower d_w/d. This plot shows data for $d_w/d = 0.25$ (diamonds), $d_w/d = 0.5$ (triangles), $d_w/d = 1.0$ (circles), and $d_w/d = 2.0$ (squares). Note that the magnitude of the normal convection at $\theta = 0$ decreases as the roughness decreases. Another effect of smoothing the walls is lowering the transition angle (θ at which $v_{mid} = 0$). These data were taken for a system like that in Fig. 5(a). (b) An increase in wall roughness leads to a higher transition angle (θ_{tr}). The crossover values from the data in (a) are plotted versus roughness.

VI. PHYSICAL MECHANISM

What characteristics of granular materials contribute to their distinct convective behavior? Why is there motion along the walls? There have been a variety of approaches to these questions. Beginning with Reynolds observations on ''dilatancy'' [35] over 100 years ago, the variation in density available to granular materials has been recognized as an important factor in explaining the range of observed behaviors. The effects of ambient gas on convection, as seen in experiments [30], suggest that studying the spaces between the particles is as important as studying the particles themselves. The formation of voids in vibrated granular systems has often been emphasized as the key to convection [29,36]. An extension to this approach is to focus on the location in the system where the voids occur, to look at the spatial variation in the granular density [1,3,4,34]. This brings to the fore the issue of the walls. It has been observed both experimentally and computationally that the condition of the walls has a large effect on the behavior of the system [4,5,20,31]. Some works also stress the role of the base of the container in producing convection rolls [32,33]. This paper will focus on the interaction between the particles and the walls as the primary force in creating convective behavior. However, the effect of granular density on this interaction will play an important role in the discussion. Almost all the previous simulational studies of granular convection focused on systems with vertical walls [37]. This section of the paper describes a physical mechanism that not only accounts for the normal convection rolls seen when $\theta = 0$, but also explains the reversal of rolls at large wall angles as well as the observed effects of varying wall roughness. The explanation of the transition from normal to reversed rolls satisfies the recent experimental challenge [7] to the models for granular convection.

A. Normal and reversed convection rolls

Convection is defined to be the net displacement of the particles over the course of one oscillation of the container. Thus, to understand the direction and magnitude of the convection, it is necessary to look at the density and motion of the grains throughout the cycle. The container goes up and down; so do the particles. What is most important are any asymmetries that occur and that may result in net shifts of the grains. Lee [4] in particular emphasizes the variation in density over the course of a cycle and the effect that it has on the shear forces exerted by the walls of the container. There are two distinct phases that make up one oscillation: when the grains are moving up relative to the container and when they are moving down. In a container with vertical walls, the particles are closely packed on the way up, but expand to a lower density on the way down. (Taguchi also points out this difference between ''forced motion'' and free fall [32].) As Lee observes, at higher densities, the sides of the container can exert a larger drag force on the particles. This means that the grains, as a whole, experience a larger pull downward in the first part of the cycle than upward in the second. This means that there is a net downward shear force exerted by the walls on the particles over the course of a cycle and this effect can explain the motion downward along the sides of the container in normal granular convection.

The conceptual backbone of the above approach is a description of convection as driven by the particles' interactions with the walls. In this picture, what is important is the density of the grains near the wall (ρ_{nw}) and their velocity relative to the container (v_{rel}). Both determine the magnitude of the force exerted and the latter determines its direction. If F_{wg} is the force on the grains from the walls, we expect that

$$F_{wg} \propto \rho_{nw}(-v_{rel}), \tag{5}$$

where the constant of proportionality is positive. The negative sign in front of v_{rel} indicates that this is a drag force and the wall-particle boundary can be thought of as a density-dependent frictional interaction. Note that Eq. (5) describes a linear dependence of the force on density and velocity. Figure 7 plots the force exerted against the product $\rho_{nw}(-v_{rel})$, where the data come from various locations in the container and various points in the cycle. Note that the trends implied by Eq. (5) are confirmed; specifically, the direction of the force is in fact always opposite that of the relative velocity. However, the assumption of linear dependence seems to be an oversimplification.

This approach works well to explain the normal convective motion in a system with vertical walls. Can it explain why the rolls reverse when the walls are pivoted outward? Again, separate an oscillation into two phases. As before, in the first part, the grains are moving upward relative to the container, so the force is downward; in the second part, the particles are moving down into the container, so the force exerted by the walls is directed upward. Note that the force under discussion is the shear force, the component of the force exerted parallel to the side of the container. When we say it is directed ''up'' we mean along the wall toward the open top of the container. Now consider the geometrical effects on density variation. Because the walls are tilted outward, as the particles rise, the horizontal space available to them increases. This means that, in the first phase of the cycle, the particles near the wall can expand into the space created as the grain pack lifts away from the walls. This in turn implies that the density near the walls will be low while the particles are moving upward. On the way down, the particles must be packed into the narrower space at the base of the container and hence the density is higher. Since the density is greater when the particles are moving downward, the magnitude of the drag force exerted during that phase of the cycle will be larger and the net force over the course of the cycle will be be upward. Therefore, the grains near the walls will be convected up along the sides. This is the origin of the roll reversal at large θ.

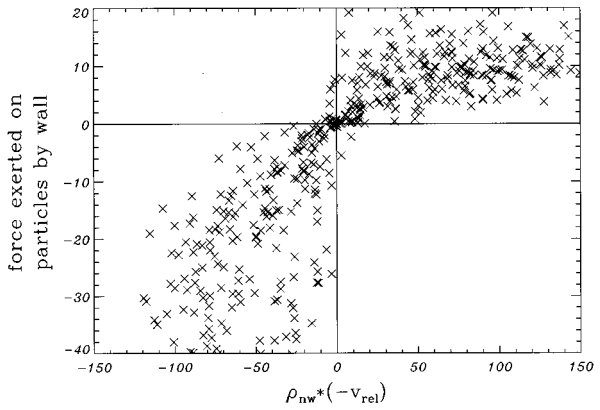

FIG. 7. Shear force exerted by the wall on the grains near the wall F_{wg} plotted against the negative of the product of the particle density near the walls and the velocity of those particles relative to the container $\rho_{nw}(-v_{rel})$. Note that the sign of the force is determined by this product; also, the force does seem to increase in magnitude as the product increases. These data are for a container with vertical walls and $d_w/d=1$. The particle density ρ_{nw}, is in the number of particles per unit area, where a unit area is the square of the radius of a particle. The relative velocity v_{rel} is in units of particle radii per cycle. The force F_{wg} is in arbitrary units, as it is actually calculated from the shift in particle momentum during a collision, under the assumption that the average particle mass and the collision time are both one, in some arbitrary units.

Note that the physical mechanism at work, density-dependent wall friction, is the same for normal and reversed rolls. What is different is where in the cycle the particles near the wall reach their minimum or maximum densities. This difference is confirmed by simulational data. Figure 8 plots the density of the grains near the wall versus time over the course of one cycle for vertical and tilted sides. Figure 8 also shows the shear velocities of those particles relative to the container (v_{rel}) over the same cycle. It is clear that for vertical walls ($\theta=0$) the density minimum occurs when the grains are moving down into the container ($v_{rel}<0$), while when the sides are tilted out ($\theta=25$), the density minimum is during the phase of the cycle when the particles are rising relative to the container ($v_{rel}>0$). These plots confirm the qualitative description of the behavior detailed in the previous paragraphs.

B. Dependence on wall roughness

As was seen in Sec. V, varying the roughness of the sides of the container has two measurable effects on convection.

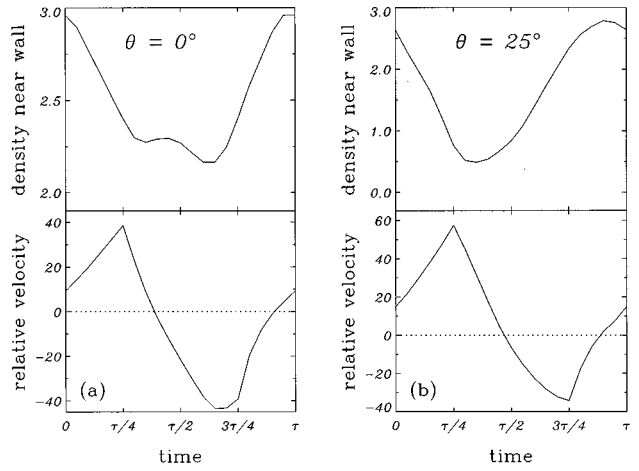

FIG. 8. Variation in the density of the grains near the wall over the course of one cycle (τ is the period of oscillation for the container). Also plotted versus time is the velocity of the particles relative to the container (v_{rel}). (a) For vertical walls ($\theta=0$) and hence normal convection rolls. Note that the density minimum occurs when $v_{rel}<0$, i.e., the particles are moving down relative to the walls. (b) For tilted out walls ($\theta=25$) and hence reversed convection rolls. Note that in this case the density minimum occurs when $v_{rel}>0$, i.e., the particles are moving up relative to the walls. The units for the density and for the relative velocity are as described in Fig. 7.

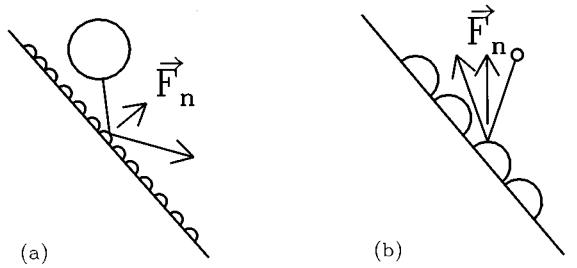

FIG. 9. Cartoon representing the different types of collisions that occur when the walls are (a) smooth (small d_w/d) and (b) rough (large d_w/d). What is important is the difference in the direction of the normal force; in (a) it is directed perpendicular to the wall, while in (b) there is a significant component along the wall.

First, the rougher walls produce stronger rolls (the magnitude of the convective velocities are larger). Second, smoother walls enhance the formation of reversed rolls, hence lowering the transition angle. Both of these effects can be explained by examining how efficiently the wall exerts force on the nearby particles and in what direction.

In hard particle collisions, most of the force is exerted in the normal direction, perpendicular to the plane of contact (i.e., along the line between the centers of the particles). In terms of the model used in these simulations, this can be seen by noting that the normal force is proportional to $1+\epsilon_n$, while the tangential force is proportional to $1+\epsilon_t$ or $\mu(1+\epsilon_n)$, both of which are smaller factors. This implies that in a collision between a wall particle and a free particle the majority of the force on the free grain is exerted perpendicular to the plane of contact.

For smooth walls, the particles glued to the walls are much smaller than the free grains. This means that the free particles cannot ''see'' the spaces between wall particles and hence most collisions between wall and free particles occur at the top of the wall particles [see Fig. 9(a)]. In this configuration, the plane of contact is parallel to the wall and hence the force is mainly exerted perpendicular to the side. For rougher walls, the free particles are much smaller than the wall particles and hence can move into the crevices and collide with any part of the wall particles [see Fig. 9(b)]. This freedom results in a range of possible orientations for the plane of contact and hence a range of directions for the normal force. Thus, while the smooth walls mainly exert a force perpendicular to themselves, the rough walls can also exert a shear force on the free particles.

The consequences of this difference are twofold. First is the effect on the magnitude of the convection rolls. Stronger rolls are produced by larger shear forces, which occur for rougher walls. Second is the effect on roll reversal. An important element in the formation of reversed rolls in the lowering of the particle density near the walls. For this to occur, the walls must push the particles away, i.e., the force must be exerted perpendicular to the sides. Since smoother walls are more efficient about exerting force in such a direction, it will be easier for reversed rolls to form; hence the transition angle will be lower in systems with smoother walls.

C. Transition between normal and reversed rolls: Behavior at intermediate wall angles

In Sec. IV, the transition from normal to reversed rolls as the wall angle increases was observed by measuring the convective velocity of the particles in the center of the container. This quantity describes the direction and strength of the convection rolls. The experiment also measures this central velocity. However, in a simulation, the convective velocity can be calculated at all points of the container. Such data describe the size and shape of the convective motion throughout the system. Figure 10 shows such flow diagrams for normal ($\theta=0$) and reversed ($\theta=25$) rolls. Using this technique, we can probe the behavior of the granular material at intermediate wall angles.

The magnitude of the force exerted by the walls depends on the granular density near the walls. Since this density varies with height, the net force exerted will also vary. This effect can be seen for vertical walls in the variation of convective velocity with height (see Sec. III). But this is just a difference in the magnitude of the force. The density variation with height can also affect the direction of the net force. The key difference between normal and reversed rolls is where over the course of an oscillation the minimum density occurs (see Fig. 8). Since the density varies with height, the location of the minimum density in time could also be different for different heights, as if a density wave was propagating through the system. Then the parts of the system where the density minimum occurred as the particles were moving down would ''feel'' a net downward shear and experience normal convection, while the other parts, where the density minimum occurred as the particles were moving up, would feel a net upward shear and hence reversed convection.

At intermediate angles, particles near the bottom of the container are limited in their expansion by the pressure from

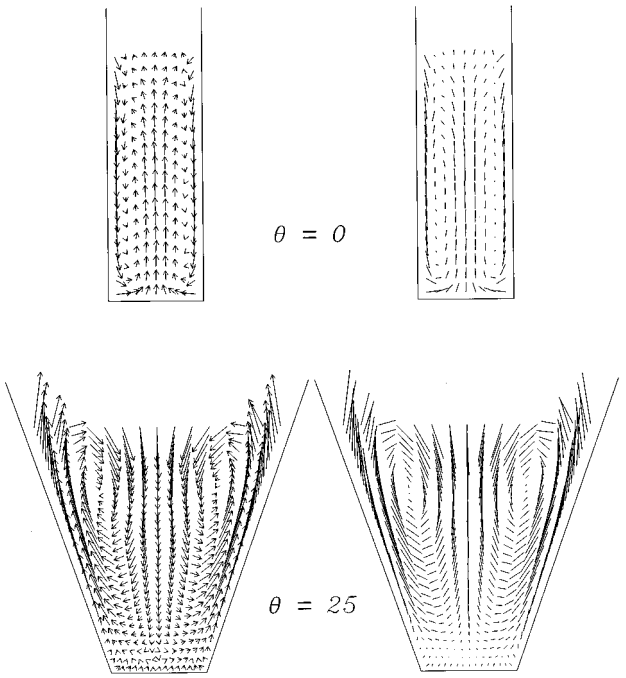

FIG. 10. Convective velocities throughout the container for normal ($\theta=0°$) and reversed ($\theta=25°$) convection rolls. There are two pictures at each angle; the second is the same as the first, but with the arrowheads removed so the shape of the rolls can be seen more clearly.

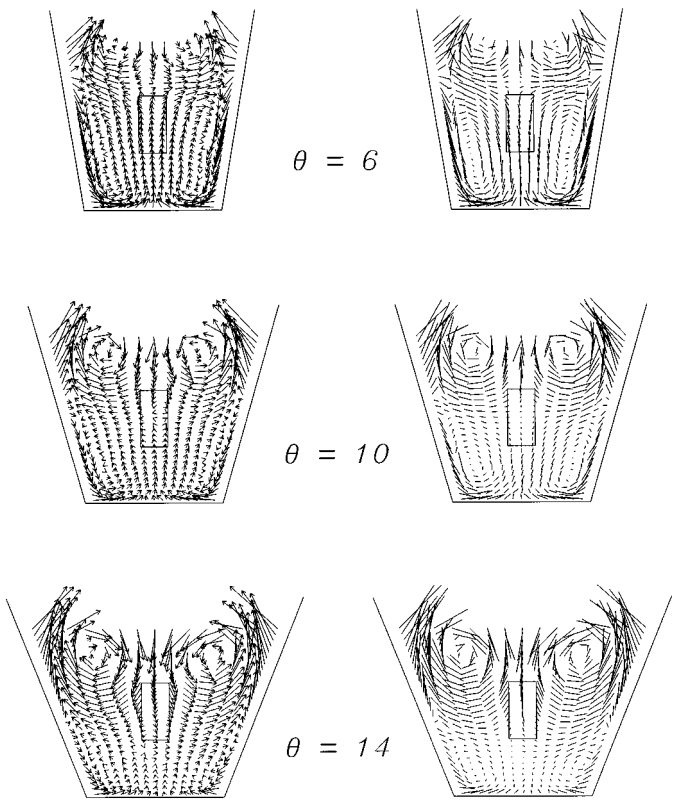

FIG. 11. The convective velocities throughout the container for intermediate angles. Note that at $\theta=6°$, normal rolls dominate the behavior, but there are small reversed rolls that have formed at the top of the container. The two types of rolls share the system equally at $\theta=10°$, but by $\theta=14°$, the reversed rolls are dominating with small remnants of normal rolls in the bottom of the container. The boxes in all the diagrams indicate the area in which v_{mid} was measured to calculate the data for Fig. 5(a).

the top part of the bead pack, while the grains near the top can expand more easily. This implies that reversed rolls form more easily at the top of the container and thus suggests that convection rolls of different directions can coexist at intermediate wall angles. The simulations confirm this phenomenon (see Fig. 11). This prediction has not yet been tested experimentally. However, there are a variety of factors that might make the coexistence of convection rolls difficult to observe. For example, both the normal and reversed rolls are rather weak at the transition angle, so the convective velocities are rather small and hence difficult to measure. Also, as density variation is an important ingredient in the mechanism described in this section, perhaps it would be easier to observe coexisting rolls in systems where less driving energy is dissipated in the bead pack and the range of densities available to the grains is increased. The energy lost in the bulk of the material can be limited by looking at smaller systems, more strongly forced systems, or less inelastic granular materials. Computational studies suggest that when ϵ_n, the normal coefficient of restitution, is increased (i.e., the system is made less ''sticky''), the range of wall angles for which coexistence is observed increases and the magnitudes of the convection velocities get larger.

Another way to emphasize the key roll that geometry plays in roll reversal is to look at how the convection changes when the container is shaken at difference frequencies. The strength of the forcing, as measured by Γ, is held constant. To summarize the data, we again plot v_{mid}, the convective velocity in the center of the system, against wall angle θ as in Sec. IV. As can be seen from Fig. 12, the transition angle is independent of frequency. However, the strength of the convection rolls decreases as the frequency

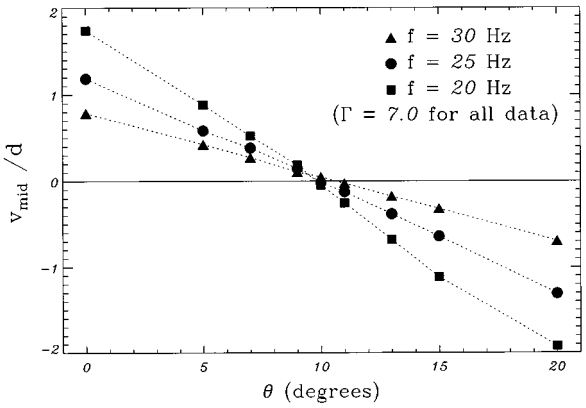

FIG. 12. Convection velocity (v_{mid}) of particles in the center of the container as a function of wall angle (θ). The strength of the forcing is the same for all data ($\Gamma=7.0$), but the frequencies of vibration are different: $f=30.0$ Hz (triangles), $f=25.0$ Hz (circles), and $f=20.0$ Hz (squares). Note that the transition angle (where $v_{mid}=0$) is the same for all three frequencies, but the strength of the convection rolls increases with decreasing frequency. The data are from a simulational system identical to that used in Fig. 5(a).

increases. For higher frequencies, the period is shorter and hence the range of densities explored by the system is narrower. As the magnitude of the net force exerted by the walls over the course of the cycle is determined by the difference between the densities on the upward and downward phases of the cycle, the smaller range produces a lower net shear and therefore weaker convection rolls. These effects of varying the frequency (the independence of the transition angle and the change in the convective velocities) are another prediction that may be tested experimentally and may be more easily observed than the coexisting convection rolls. For vertical walls ($\theta=0$), experiments have already demonstrated that lower frequencies produce larger convection velocities [6].

VII. CONCLUSION

In this paper, we have studied the reversal of convection rolls in vibrated granular materials. Computer simulations were shown to reproduce experimental results [6,7] both qualitatively and quantitatively. Specifically, velocity profiles of normal convection in three-dimensional systems were mimicked by two-dimensional simulations. In addition, the experimentally measured reversal of the direction of the convection rolls as the walls of the container are tilted outward was seen in the simulations as well; the angle at which this transition occurs is 10° in both systems. The effects of wall preparation on the magnitude and direction of granular convection are also reproduced in the simulations.

A possible explanation for the range of observed behaviors is discussed. The key ingredient of the proposed mechanism is a density-dependent frictional interaction between the walls of the container and nearby particles. This approach is a logical extension of previous works [4,29,34,36] that emphasize the formation of voids as a key element in accounting for granular convection. Such a view is closely related to this paper's approach that density variation throughout the bead pack is responsible for not only the existence of convection rolls, but also their reversal. Application of this model of convection to the system at intermediate wall angles suggests that the transition is marked by the coexistence of normal and reversed rolls in the same system. This prediction is confirmed by the simulations and can be tested experimentally. The model and the simulations also predict how changing the frequency of the vibrations will affect the magnitude and direction of the convection.

The behavior of a granular system will depend in a nontrivial way on system parameters, such as the strength of the forcing and the filling height, as well as on boundary conditions, such as the angle of the walls and their degree of roughness. All these inputs, as well as other characteristics, such as the hardness of the particles and the friction between them, combine to affect the range of granular densities explored during a cycle and the motion of the bead pack relative to the walls and hence the net shear force exerted by the walls on the particles. It is this force that determines the strength and direction of the convection rolls. A formula that would allow one to predict precisely the motion from the input parameters and boundary conditions is a topic for further study.

ACKNOWLEDGMENTS

I am indebted to Jim Knight and Heinrich Jaeger for stimulating my interest in this problem. I am also grateful to Sue Coppersmith, Michael Brenner, Sid Nagel, and Leo Kadanoff for their advice and many useful discussions. This work was supported by the National Science Foundation under Grant No. DMR-9415604 and the MRSEC Program, Grant No. DMR-9400379. It was also partially supported by the AASERT program of the Office of Naval Research under ONR-AASERT Contract No. N00014-94-1-0798.

[1] A. Mehta and G. C. Barker, Phys. Rep. **57**, 383 (1994).
[2] H. M. Jaeger, S. R. Nagel, and R. P. Behringer, Phys. Today **49**(4), 32 (1996).
[3] C. Laroche, S. Douady, and S. Fauve, J. Phys. (France) **50**, 699 (1989).
[4] Jysoo Lee, J. Phys. A **27**, 257 (1994).
[5] J. B. Knight, H. M. Jaeger, and S. R. Nagel, Phys. Rev. Lett. **70**, 3728 (1993).
[6] J. B. Knight, E. E. Ehrichs, V. Y. Kuperman, J. K. Flint, H. M. Jaeger, and S. R. Nagel, Phys. Rev. E **54**, 5726 (1996).
[7] J. B. Knight, Phys. Rev. E **55**, 6016 (1997).
[8] A. Mehta and J. M. Luck, Phys. Rev. Lett. **65**, 393 (1990).
[9] F. Melo, P. Umbanhowar, and H. L. Swinney, Phys. Rev. Lett. **72**, 172 (1994).
[10] Y. D. Lan and A. D. Rosato, Phys. Fluids **7**, 1818 (1995).
[11] H. K. Pak and R. P. Behringer, Nature (London) **371**, 231 (1994).
[12] J. Schafer, S. Dippel, D. E. Wolf, J. Phys. (France) I **6**, 5 (1996).
[13] N. V. Brilliantov, F. Spahn, J.-M. Hertzsch, and T. Pöschel, Phys. Rev. E **53**, 5382 (1996).
[14] O. R. Walton, Lawrence Livermore National Laboratory Report No. UCID-20297-88-1, 1988 (unpublished).
[15] S. F. Foerster, M. Y. Louge, H. Chang, and K. Allia, Phys. Fluids **6**, 1108 (1994).
[16] P. K. Haff and B. T. Werner, Powder Technol. **48**, 239 (1986).
[17] S. McNamara and J.-L. Barrat Phys. Rev. E **55**, 7767 (1997).
[18] I. Goldhirsch and G. Zanetti, Phys. Rev. Lett. **70**, 1619 (1993).
[19] S. Luding, J. Duran, E. Clement, and J. Rajchenbach, J. Phys. (France) I **6**, 823 (1996).
[20] J. A. C. Gallas, H. J. Herrmann, T. Pöschel, and S. Sokolowski, J. Stat. Phys. **82**, 443 (1996).
[21] S. Luding, E. Clement, A. Blumen, J. Rajchenbach, and J. Duran, Phys. Rev. E **50**, 4113 (1994).
[22] B. Bernu and R. Mazighi, J. Phys. A **23**, 5745 (1990).
[23] S. McNamara and W. R. Young, Phys. Rev. E **50**, 28 (1994).
[24] S. McNamara and W. R. Young, Phys. Rev. E **53**, 5089 (1996).
[25] N. Schörghofer and T. Zhou, Phys. Rev. E **54**, 5511 (1996).
[26] P. Deltour and J.-L. Barrat, J. Phys. (France) I **7**, 137 (1997).
[27] M. Nakagawa, S. A. Altobelli, A. Caprihan, E. Fukushima, and

E.-K. Jeong, Exp. Fluids **16**, 54 (1993).
[28] E. E. Ehrichs, H. M. Jaeger, G. S. Karczmar, J. B. Knight, V. Y. Kuperman, and S. R. Nagel, Science **267**, 1632 (1995).
[29] T. Shinbrot, D. V. Khakhar, J. J. McCarthy, and J. M. Ottino Phys. Rev. E **55**, 6121 (1997).
[30] H. K. Pak, E. Van Doorn, R. P. Behringer, Phys. Rev. Lett. **74**, 4643 (1995).
[31] E. Clement, J. Duran, and J. Rajchenbach, Phys. Rev. Lett. **69**, 1189 (1992).
[32] Y.-H. Taguchi, Phys. Rev. Lett. **69**, 1367 (1992).
[33] J. A. C. Gallas, H. J. Herrmann, and S. Sokolowski, Phys. Rev. Lett. **69**, 1371 (1992).
[34] M. Bourzutschky and J. Miller, Phys. Rev. Lett. **74**, 2216 (1995).
[35] O. Reynolds, Philos. Mag. **20**, 469 (1885).
[36] J. Duran, T. Mazozi, E. Clement, and J. Rajchenbach, Phys. Rev. E **50**, 5138 (1994).
[37] The main exception is Bourzutschky and Miller, who observe roll reversal when numerically solving a hydrodynamical description of the granular system.